

# INCREASED mc-Si MODULE EFFICIENCY USING FLUORESCENT ORGANIC DYES: A RAY-TRACING STUDY

Keith R. McIntosh and Bryce S. Richards

Centre for Sustainable Energy Systems, The Australian National University, Canberra, ACT 0200, AUSTRALIA  
Tel: +61-2-6125-8966, Fax: +61-2-6125-0506, Email: keith.mcintosh@anu.edu.au

## ABSTRACT

Ray tracing is used to determine how the inclusion of BASF's fluorescent organic dyes might benefit a multicrystalline silicon module. These dyes absorb short-wavelength photons and re-emit them at wavelengths that are longer and more favourable to the module. This down-shifting prevents many photons from being absorbed by the ethylene vinyl acetate (EVA) encapsulant, the cells' antireflective coating, and the "dead layer" of the cells' emitter. We find that under one-sun AM1.5g illumination, the inclusion of organic dyes might raise the short-circuit current density by as much as  $0.7 \text{ mA/cm}^2$ , which equates to an efficiency boost of 0.3% absolute. A further increase of  $0.1 \text{ mA/cm}^2$  is attained by thickening the antireflective coating so that it is optimised for the new spectrum. It is shown that the incorporation of fluorescent dyes slightly increases the optimal emitter doping of the solar cells.

## INTRODUCTION

In 1979, Hovel *et al.* concluded that the incorporation of fluorescent molecules into a silicon PV module could raise its efficiency by 0.5–2% (absolute) [1]. The reason for the boost in efficiency is that the molecules absorb photons of a short wavelength at which the modules have a low quantum efficiency, and re-emit photons at a longer, more favourable wavelength.

The development of fluorescent PV modules has been hampered by photo-instability in the case of organic dye molecules, and expense in the case of inorganic molecules. However, BASF (Ludwigshafen, Germany) has developed a range of photostable fluorescent organic dyes [2,3], providing us with a new opportunity to explore the potential of fluorescent PV modules.

In Ref. 4, the potential for including BASF's organic dyes in a thin-film PV technology is discussed. In this paper, we give a detailed examination including the dyes in planar multicrystalline silicon (mc-Si) solar cells. There are two reasons for choosing this conventional module technology: firstly, it comprises half of the world's PV production [5]; and secondly, its short-wavelength response is relatively poor, thereby providing a good opportunity to benefit from fluorescent organic dyes.

The investigation involves the ray-tracing simulation of mc-Si modules and a re-optimisation of the cell design to maximise the benefit from fluorescent dyes. Like Maruyama *et al.* [6], who investigated the effect of similar dyes on a low-efficiency mc-Si modules (<9%), we conclude that fluorescent organic dyes have the potential to increase the module efficiency by ~2.5% (relative).

## LOSS MECHANISMS IN CONVENTIONAL PV MODULES UNDER SHORT-WAVELENGTH LIGHT

There are five mechanisms that impair the short-wavelength response of a conventional PV module: (i) absorption in the glass, (ii) absorption in the ethylene vinyl acetate (EVA) encapsulant, (iii) absorption in the antireflective coating (ARC), (iv) reflection from the ARC, and (v) recombination in the emitter. Reflection from the air-glass interface and reflection from the metal grid are omitted from this list, since they constitute broadband effects.

Figure 1 plots the five losses of a PV module with planar mc-Si cells. These curves have been simulated by assuming the module to be encapsulated by 3 mm of low-iron soda-lime glass and 0.5 mm of EVA, to have an ARC composed of 75 nm of silicon nitride, and to contain cells with a  $40 \Omega/\text{sq}$  emitter; more details of the modelling are provided later.

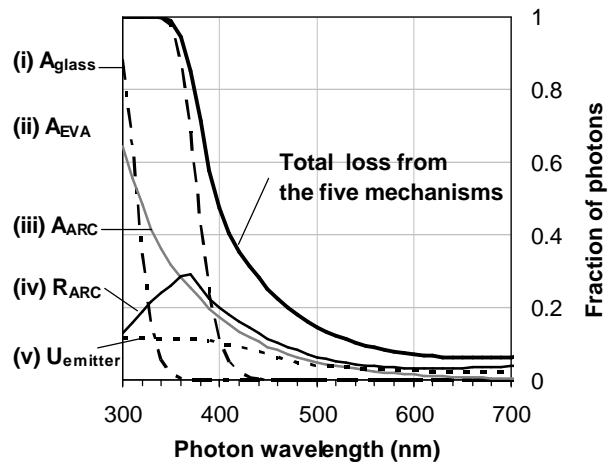


Fig. 1: Five loss mechanisms in a conventional mc-Si PV module.

Table 1: BASF dye mixtures used in this study.

Mix	Dyes	Absorption range (nm)	Emission range (nm)
	None	—	—
A	Violet570	300–410	395–500
B	A + Yellow083	300–490	470–585
C	B + Orange240	300–530	510–625
D	C + Red300	300–600	565–705

Figure 1 also plots the total loss from the five mechanisms. It shows that very few photons with wavelengths less than 400 nm contribute to the module's output, largely due to EVA absorption; when illuminated by the one-sun AM1.5g spectrum, this equates to 1.0 mA/cm<sup>2</sup> of lost current. There is also considerable loss of photons in the 400–500 nm range due to the ARC and emitter; while the fraction of lost photons is smaller, the photon flux is higher in this part of the AM1.5g spectrum, and the losses equate to 1.3 mA/cm<sup>2</sup>.

It is clear that there is much to be gained from down-shifting photons of 300–500 nm to longer wavelengths such as 600–700 nm. This down-shifting can be achieved by fluorescent organic dyes.

#### FLUORESCENT ORGANIC DYES AND THEIR INCLUSION INTO PV MODULES

Fluorescent organic dyes typically have one or two sharp absorption peaks and the same number of emission peaks at a slightly longer wavelength. In this work, we use the absorption and emission curves provided by BASF for dyes suspended in polymethylmethacrylate (PMMA) [2].

As described in Ref. 4, it is possible to dissolve multiple dyes into PMMA to attain a wide absorption band while maintaining a short emission band. In this work, we investigate four mixtures that might prove beneficial to conventional PV modules. Table 1 summarises these mixtures, where the absorption range defines the wavelengths at which the optical density exceeds 0.5, and the emission range defines the wavelengths at which the emission probability exceeds 10% of the peak emission probability. The concentration of each dye is such that its maximum optical density is 4.

While the inclusion of fluorescent dyes has the advantage of down-shifting photons to favourable wavelengths, it has the disadvantage of introducing new loss mechanisms, much of which relate to their isotropic emission of photons. Most significantly, when dyes emit from within PMMA or glass ( $n = 1.5$ ), about 12.5% of the emitted rays are within the escape cone of the glass–air interface [1] and are therefore lost from the module. Isotropic emission also leads to many rays being propagated at angles that are oblique to the plane of the cells; compared to perpendicular light, these rays suffer more absorption in the glass and EVA, and more

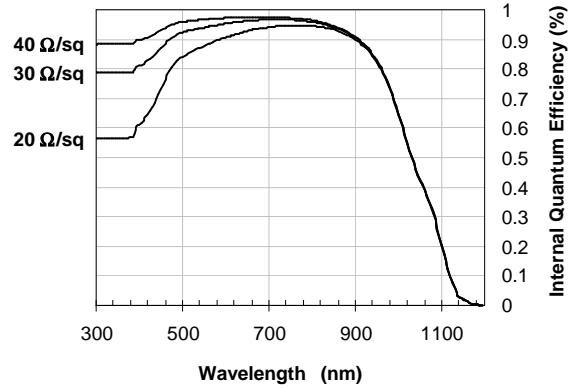


Fig. 2: IQE vs wavelength for three emitter sheet resistances (PC1D modelling).

absorption and reflection by the ARC. A third source of loss arises when a dye's luminescence quantum efficiency (LQE) is less than unity; i.e., when a dye does not always emit a photon after absorbing one. In this study, the dyes' LQEs were measured by BASF to be Violet570: 93%; Yellow083: 99%; Orange240: 100%; and Red300: 98%.

To determine whether the advantage of down-shifting outweighs these additional losses, we performed ray-tracing simulation.

#### INPUTS TO RAY TRACING

Simulations were performed using an in-house ray tracer called *Raylene*. *Raylene* tracks the position, direction, intensity and wavelength of rays as they pass through the module. Following standard optical laws, it determines the losses associated with absorption in the glass, EVA and silicon nitride (SiNx) ARC, and reflection at all interfaces.

The refractive index and absorption coefficient of the glass (B270), EVA and SiNx (RPECVD2) were taken from Nagel *et al.* [7]; these parameters were used to determine reflection at the air–glass and EVA–SiNx interfaces, and absorption in the glass, EVA and SiNx. An additional 5% broadband reflectance was added to the EVA–SiNx interface to represent reflection from the metal grid. All interfaces were assumed planar, parallel and specular and the thickness of the glass and EVA was set to 3 and 0.5 mm, respectively.

To simulate the response of the solar cells to incident light, an internal quantum efficiency (IQE) was generated as a function of wavelength using PC1D [8]. Fig. 2 shows the IQE that was generated for three sheet resistances, where the bulk was 300 μm thick, 1.5 Ω-cm *p*-type, with a carrier lifetime of 50 μs. The surface recombination velocity at the front and rear surfaces was set to 10<sup>3</sup> and 10<sup>7</sup> cm/s. And the material parameters were kept at PC1D's default values for silicon. Note that the IQEs of Fig. 2 omit the effect of absorption in the SiNx because it is already accounted for in the optical modelling.

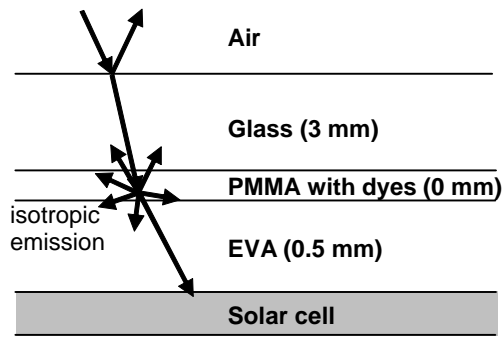


Fig. 3: Schematic diagram of ray-tracer model illustrating an absorption–emission event by a fluorescent dye.

Reflection from between cells was neglected, as were losses at the edge of the module; these effects have little impact on the comparison at hand.

Interactions between the rays and the organic dye molecules were accounted for by using the emission and absorption spectra provided by BASF [2]. The emission was isotropic and the ray intensity was reduced by the dye’s LQE as listed earlier. The ray tracer assumed that the dyes are suspended in a negligibly thin layer of PMMA between the glass and EVA, as illustrated by Fig. 3. (Practically, the PMMA layer might be applied to the back side of the glass by a spray-coating process; between the glass and EVA it is protected from the elements.)

The incident light was perpendicular to the module and represented one-sun illumination (AM1-5g). Convergence to 0.05 mA/cm<sup>2</sup> was attained by tracing 100,000 incident rays.

## RESULTS

Without any optimisation of the cell design, the inclusion of Mix B increased the short-circuit current density  $J_{sc}$  from 31.4 to 32.1 mA/cm<sup>2</sup>; this equates to the module efficiency increasing from 14.8 to 15.1%. Most of this improvement comes from a reduction in EVA absorption.

An additional increase of 0.1 mA/cm<sup>2</sup> was attained by raising the silicon nitride thickness from 75 to 85 nm. A thicker SiNx shifts the reflection minima to longer wavelengths, which is better suited to the spectrum that is incident on the cells. The dependence of  $J_{sc}$  on nitride thickness is shown by Table 2 and Fig. 4; notice that the optimal nitride thickness increases as the dyes’ emission range increases.

Figure 5 plots the external quantum efficiency of the module as determined by the ray tracer. It compares the response of a module with no dyes to that with the greatest gain in  $J_{sc}$  (Mix B, 85 nm SiNx). It demonstrates that the module with Mix B responds to shorter-wavelength photons. As described earlier, this is because

Table 2: Optimum SiNx thickness and  $J_{sc}$ .

Mix	Dyes	optimal SiNx thickness (nm)	Max $J_{sc}$ (mA/cm <sup>2</sup> )
	None	74	31.4
A	Violet570	77	31.8
B	A + Yellow083	82	32.2
C	B + Orange240	86	32.1
D	C + Red300	90	31.7

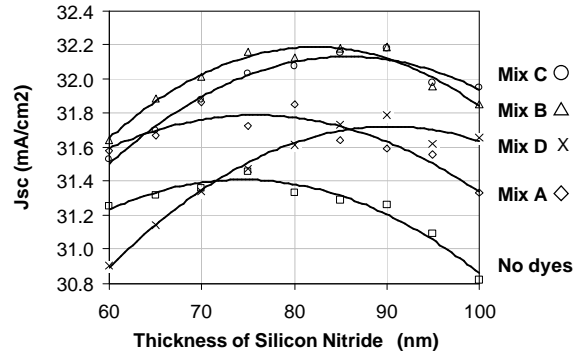


Fig. 4: Simulated  $J_{sc}$  (symbols) with quadratic fits (lines) as a function of SiNx thickness.

the organic dyes absorb short-wavelength photons before they are absorbed by the EVA, and re-emit them at longer, more favourable wavelengths. Also note that EQE of the “Mix B” module is slightly better in the range 650–1000 nm due to its thicker SiNx.

As well altering the optimum ARC thickness, the inclusion of fluorescent dyes might also alter the optimal emitter doping. In conventional mc-Si solar cells, the emitter sheet resistance is ~40 Ω/sq; the doping cannot be lower or the cell suffers from high emitter resistance, high recombination at the metal–silicon interface, high contact resistance, and high shunting; and the doping cannot be much higher or the “dead layer” at the front surface becomes too prominent. This is a well-known

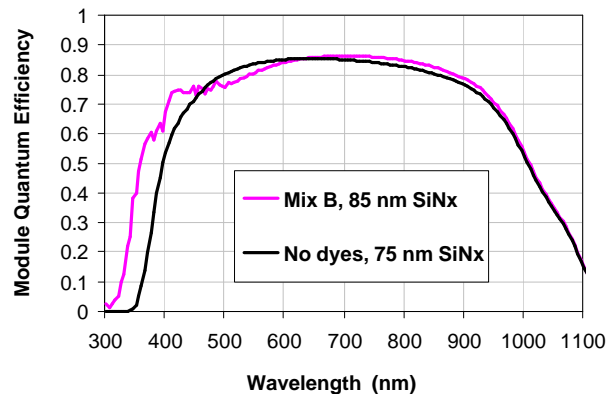


Fig. 5: Module EQE vs wavelength as determined by the ray tracer for a conventional mc-Si module with no dyes and with Mix B.

trade-off in the design of screen-printed solar cells.

It is difficult to determine the optimal sheet resistance through simulation alone because the vagaries of manufacturing have a significant effect on shunting and contact resistance. It is possible, however, to quantify the effect of recombination in the “dead layer”, thereby investigating the lower limit to the sheet resistance.

The “dead layer” is the heavily doped silicon close to the surface of the emitter; in this region, the doping is so high that minority carriers recombine before they are collected by the junction. Fig. 2 plots the IQE of a mc-Si solar cell as modelled with PC1D; it illustrates how carrier collection becomes poorer as the sheet resistance decreases, and how the “dead layer” has a greater influence on shorter-wavelength photons (since they are more likely to be absorbed near the front surface).

When the emitter doping is increased, the IQE decreases at all wavelengths and hence, irrespective of any fluorescent dyes, the  $J_{sc}$  decreases. The decrease in  $J_{sc}$  is, however, somewhat mitigated by fluorescent down-shifting.

Figure 6 plots  $J_{sc}$  vs emitter sheet resistance. The figure shows that when the emitter sheet resistance is reduced from 40 to 30  $\Omega/sq$ , the  $J_{sc}$  of a module with no dyes would reduce by 0.6  $mA/cm^2$ ; by comparison, the  $J_{sc}$  of a module with mix C would reduce by 0.4  $mA/cm^2$ .

It can be concluded, therefore, that when fluorescent dyes are incorporated in the module, there is slightly less recombination in the “dead layer”. Consequently, the optimal sheet resistance must be slightly reduced. This might have beneficial consequences for manufacturing since, generally, heavier doped emitters lead to a more robust process.

## CONCLUSION

Ray tracing was used to evaluate the performance of a multi-crystalline silicon module whose encapsulation incorporates BASF's fluorescent organic dyes. It was found that under one-sun AM1.5g illumination, the inclusion of organic dyes raised the short-circuit current density by 0.7  $mA/cm^2$ , which equates to an efficiency boost of 0.3% absolute. A further increase of 0.1  $mA/cm^2$  was attained by thickening the antireflective coating so that it is optimised for the new spectrum incident to the cells. It was also shown that the incorporation of fluorescent dyes will slightly increase the optimal emitter doping of the solar cells in the module.

## ACKNOWLEDGEMENTS

This work is funded under a research contract between BASF and the ANU. We thank Arno Boehm, Axel Grimm, Alfred Rennig, Martin Koenemann and Christian Lach from BASF for contributing data and their knowledge of fluorescent dyes.

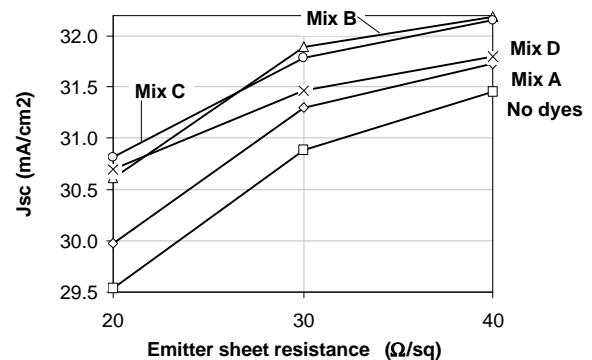


Fig. 6: Simulated  $J_{sc}$  vs emitter sheet resistance.

## REFERENCES

- [1] H.J. Hovel *et al.*, *Solar Energy Materials*, **2**, pp. 19–29, 1979.
- [2] Lumogen F series organic dye data sheets, [http://www.basf.de/en/produkte/farbmittel/farben/pigmente/plastics/farbmittel/farbstoffe/?sortiment=Lumogen+F&db\\_id=28&id=QI9JZ7otEbcp0ka](http://www.basf.de/en/produkte/farbmittel/farben/pigmente/plastics/farbmittel/farbstoffe/?sortiment=Lumogen+F&db_id=28&id=QI9JZ7otEbcp0ka)
- [3] G. Seybold and G. Wagenblast, *Dyes and Pigments* **11**, pp. 303–317, 1989.
- [4] B.S. Richards and K.R. McIntosh, “Enhancing the efficiency of production CdS/CdTe PV modules by overcoming poor spectral response at short wavelengths via luminescence down-shifting”, *Proc. of 4th WCPEC*, Hawaii, 2006.
- [5] *PHOTON International*, p. 74, March 2005.
- [6] T. Maruyama *et al.*, *Solar Energy Materials & Solar Cells* **64**, pp. 269–278, 2000.
- [7] H. Nagel, A.G. Aberle and R. Hezel, *Progress in Photovoltaics*, **7**, pp. 245–260, 1999.
- [8] P.A. Basore and D.A. Clugston, “PC1D version 4 for windows: From analysis to design”, *Proc. 25th IEEE PVSC*, Washington, pp. 211–214, 1996.